
Published article:

Dou, B, Dupont, V, Rickett, G, Blakeman, N, Williams, PT, Chen, H, Ding, Y and Ghadiri, M (2009) *Hydrogen production by sorption-enhanced steam reforming of glycerol.* Bioresource Technology, 100 (14). 3540 - 3547.

http://dx.doi.org/10.1016/j.biortech.2009.02.036

Hydrogen Production by Sorption-Enhanced Steam Reforming of Glycerol

Binlin Dou, Valerie Dupont*, Gavin Rickett, Neil Blakeman, Paul T. Williams,

Haisheng Chen, Yulong Ding, Mojtaba Ghadiri

School of Process, Environmental and Materials Engineering, University of Leeds,

Leeds, LS2 9JT, UK

Corresponding author: V.Dupont@leeds.ac.uk

Paper accepted and published. Full reference:

Binlin Dou, Valerie Dupont, Gavin Rickett, Neil Blakeman, Paul T. Williams, Haisheng Chen, Yulong Ding, Mojtaba Ghadiri. Hydrogen Production by Sorption-Enhanced Steam Reforming of Glycerol. Bioresource Technology, 100 (2009), 3540-3547

Abstract: Catalytic steam reforming of glycerol for H_2 production has been evaluated experimentally in a continuous flow fixed-bed reactor. The experiments were carried out under atmospheric pressure within a temperature range of 400-700°C. A commercial Ni-based catalyst and a dolomite sorbent were used for the steam reforming reactions and *in-situ* CO_2 removal. The product gases were measured by online gas analyzers. The results show that H_2 productivity is greatly increased with increasing temperature and the formation of methane by-product becomes negligible above 500°C. The results suggest an optimal temperature of ~500°C for the glycerol steam reforming with *in-situ* CO_2 removal using calcined dolomite as the sorbent, at which the CO_2 breakthrough time is longest and the H_2 purity is highest. The

---

[*] Author to whom correspondence should be addressed. Tel: 44 -113-3432503; Fax: 44 -113-2467310, v.dupont@leeds.ac.uk.

shrinking core-model and the 1D diffusion model describe well the CO_2 removal under the conditions of this work.

Keywords: Sorption-enhanced steam reforming; Glycerol; Hydrogen.

1. Introduction

Growing environmental concerns and energy demands worldwide have caused the use of biodiesel and its production to gain momentum. About 10 wt% of glycerol is produced during the conversion of vegetable oils or animal fats into biodiesel fuel through the catalytic transesterification process (Ma, et al., 1999). The glycerol by-product is now in surplus and could even become a waste problem. As hydrogen is an ideal clean energy, conversion of glycerol to hydrogen is one of the most attractive ways to make use of glycerol, as it can theoretically produce up to 4 mol of hydrogen gas (from its molecular formula of $C_3H_5(OH)_3$). This makes hydrogen generation from biomass derived glycerol a potentially economically viable and environmentally friendly option.

The catalytic steam reforming of glycerol to produce hydrogen may be considered to occur first through glycerol dehydrogenation. This leaves CO bonded onto the catalyst surface, which could then undergo desorption, followed by water-gas-shift or methanation (Slinn, et al., 2008). Some studies have been carried out on glycerol steam reforming for hydrogen production. Czernik et al. (Czernik, et al., 2002) studied the hydrogen generation by steam reforming of biomass-derived liquids over a commercial nickel based naphtha reforming catalyst (C11-NK). Such a catalyst was chosen due to its high activity and low cost. Adhikari et al. (2007a) carried out a thermodynamic equilibrium analysis of hydrogen production by steam reforming of glycerol. They calculated the number of moles of hydrogen produced on the basis of minimising the Gibbs function. Their results showed high temperatures, low pressures, and high ratios of water-to-glycerol feed favoured the hydrogen production. A statistical approach to study the reforming of glycerol to produce hydrogen using a fixed bed reactor of nickel-based catalyst was carried out by Douette et al. (2007), who examined the effects of the reformer temperature, oxygen to carbon ratio, and steam to carbon ratio. Hirai et al. (2005) reported that glycerol steam reforming over a Ru/Y_2O_3 catalyst exhibited a H_2 selectivity of about 90% and complete conversion of glycerol at 600°C. Zhang et al. (2007) produced H_2 through the glycerol steam reforming over ceria-supported metal catalysts and found that a glycerol conversion of 100% could be achieved at 400°C. Adhikari et al. (2007b) studied steam reforming of glycerol using an alumina-supported metal catalyst over a range of conditions and showed that, at high temperatures, high gas yield was reached and selectivity of up to 70% was obtained. Steam reforming of glycerol was evaluated on Ni/CeO_2, Ni/MgO, and Ni/TiO_2 catalysts (Hirai, et al., 2005). The results show that Ni/CeO_2 is the best catalyst, which gives a H_2 selectivity of 74.7% and a glycerol conversion of 99% at 600°C. In our previous work, the simulation of gas-solid flow and H_2 production during the steam reforming of glycerol in a fluidised bed reactor was also carried out (Dou, et al., 2008).

One of the difficulties associated with the utilization of the syngas produced by steam reforming for energy production is the high CO_2 and CO contents. Especially for all fuel cell systems, large CO_2 content of the fuel gas greatly drops the efficiency of the system, whereas CO has very strong poisoning effect on the catalyst of PEMFC (Lee, et al., 2008). The conventional CO_2 and CO cleanup from the steam reforming reactor is a very costly and complicated process (Harrison, 2008). Within the last few years a new concept involving simultaneous hydrogen production and carbon dioxide removal has been proposed, and the steam reforming processes could be enhanced through both reforming and water-gas shift reactions. Generally, an integral fixed-bed reactor with a mixture of the steam reforming catalyst and solid sorbent to selectively remove CO_2 is used. This process is well known as the sorption-enhanced reaction process and has been widely studied by steam methane reforming (Mayorga, et al., 1999; Ding, et al., 2000; Balasubramanian, et al., 1999; Kinoshita, et al., 2003; Yi, et al., 2005; Lee, et al., 2007; Li, et al., 2007; Essaki, et al., 2008; Harrison, 2008). For example, Balasubramanian et al. (1999) reported on H_2 production through sorption-enhanced reaction process using a laboratory-scale fixed bed reactor containing a reforming catalyst and CaO formed by calcination of high-purity $CaCO_3$, the results of which showed that a gas with a hydrogen content up to 95 % (dry basis) could be produced. Essaki et al. (2008) studied the effect of equilibrium shift in methane steam reforming by a reactor of 21 mm diameter with a mixture of 10g reforming catalyst and 60g CO_2 sorbent. The results showed the H_2 concentration reached 93.6 vol% and CO concentration was below 0.2 vol% at 550 °C. Kinoshita and Turn (2003) investigated the simulation of hydrogen production from bio-oil steam reforming by the sorption enhanced reforming process. The use of such process greatly decreases the CO_2 concentration and increases hydrogen purity. In addition, the capital cost can be reduced as the number of processing steps required for subsequently separating CO_2 is removed (Hufton, et al., 1999; Balasubramanian, et al., 1999; Yi and Harrison, 2005; Harrison, 2008). Some studies also showed that CO_2 sorption enhancement enables the use of a lower reaction temperature, which may reduce energy usage and catalyst sintering. At the same time, it is possible for the steam reforming process to use less expensive reactor materials (Ding, et al., 2000; Lee, et al., 2007; Essaki, et al., 2008; Harrison, 2008).

To date, although there have been a few studies on the use of catalysts active for methane and/or ethanol steam reforming such as Ni-based catalysts for steam reforming of glycerol (Adhikari, et al., 2007a; 2007b and 2008; Czernik, et al., 2002; Douette, et al., 2007; Hirai, et al., 2005; Zhang, et al., 2007), little has been found in the literature on glycerol steam reforming with *in-situ* CO_2 removal. This forms the main motivation for carrying this study on the use of a commercial Ni-based catalyst and a calcined dolomite sorbent to investigate the feasibility of sorption enhanced steam reforming of glycerol for hydrogen production. A fixed-bed reactor was employed. Experiments using the catalyst only, i.e., without sorbent, were also carried out for comparison. The whole fixed bed reactor was placed in a temperature-controlled oven, which allowed effect of the temperature to be investigated.

2. Experimental

2.1 Materials

The catalyst was a commercial Ni-based steam reforming catalyst manufactured by Johnson Matthey. It was in the form of cylindrical pellets with 0.0138 m diameter, 0.0184 m height, perforated with four equidistant holes of 3.8×10^{-3} m diameter. The catalyst contained ca. 18 wt% NiO supported on an Al_2O_3 substrate. To remove the mass transfer effect, the catalyst was crushed to $(0.66\text{-}1.70)\times10^{-3}$ m size range for the experiments. Dolomite from the Warmsworth quarry (Yorkshire, UK), was chosen for the *in-situ* CO_2 removal because of its low cost and high CO_2-capacity. More importantly, the sorbent did not contain components that poisoned the catalyst, e.g. sulphur, and had been used in previous studies of steam reforming of methane and vegetable oil (Dupont et al., 2007 and 2008). The dolomite consisted of MgO 21.3 wt%, CaO 30.7 wt%, SiO_2 0.3 wt%, Fe_2O_3 0.27 wt% and Al_2O_3 0.1 wt%. Prior to the experiments, dolomite was calcined at 850°C for at least 4 hr to obtain the desired oxidised form. Previous studies indicated that once calcined, MgO in the dolomite was no longer able to carbonate and only the CaO component remained active as a CO_2 sorbent. The calcined dolomite was also crushed to $(0.66\text{-}1.70)\times10^{-3}$ m size for the experiments.

A higher resolution scanning electron microscopy (SEM) (LEO 1530) coupled to energy dispersive X-ray spectrograph (EDXS) was used to study the morphology of the fresh, reduced and spent catalyst. Glycerol of 99.10% purity purchased from Sigma-Aldrich Inc (G6279) was used in the experiments.

2.2 Experimental set-up

Figure 1 shows a schematic diagram of the laboratory system used for the catalytic steam reforming of glycerol. The system consisted of a continuous flow fixed-bed reactor placed in an oven with temperature control. The reactor had an internal diameter (ID) of 0.025 m and was 0.70 m long. There was an injector in the lower part of the reactor for supplying the reactants. The injector had an ID of 10^{-3} m and was 0.28 m long. Two K-type thermocouples were used to measure the injector outlet temperature and the catalyst bed temperature. The experiments were carried out at a temperature range of 400-700°C under atmospheric pressure. Gases from high pressure cylinders, regulated by MKS mass flow controllers with a four-channel readout, were mixed to predetermined inlet gas compositions. A nitrogen flow of 0.5×10^{-3} m^3 min^{-1} (STP) served as a carrier and aided in elemental and mass balance analyses to determine reactants conversions and products yield and selectivity for the runs where the CO_2-sorbent was not used. A sample of 5 g of catalyst with or without 5 g of sorbent was loaded into the reactor supported by a circular mesh screen in the bottom part of the reactor. Before each run, the catalyst was reduced with a continuous flow of 5 vol% H_2 mixed with 0.5×10^{-3} m^3 min^{-1} (STP) N_2 at 400°C for 2 hours. Liquid glycerol/water mixture with a preset ratio was then injected by a micro-syringe pump into the injector. As the injector was housed in the furnace, the mixture was heated above 300°C to vaporise it and was subsequently mixed with the diluting N_2 stream at a position of 0.02-0.03 m below the catalyst bed. The feed gas composition of glycerol/H_2O/N_2 was kept at 1.25/11.25/87.5 vol%, achieving a steam to carbon (S/C) ratio of 3. The outlet product gas from the condenser was analyzed for its H_2, CO, CO_2 and CH_4 concentrations with an ABB on-line gas analysers rack of Advance Optima AO2000 Series (Uras 14 for CO, CO_2 and CH_4, and Caldos 15 for H_2).

2.3. Reactions and Formulae for the data analyses

Reforming reactions are generally highly endothermic, and a catalyst is often required to accelerate the reactions and favour hydrogen production in the reforming process (Adhikari, et al., 2008). The catalytic steam reforming of glycerol for hydrogen production involves complex reactions but these can be summarised by the mechanism outlined as follows.

First, the decomposition of glycerol into syngas:

$$C_3H_8O_3 \xrightarrow{H_2O} 3CO + 4H_2 \tag{R1}$$

Followed by the water-gas shift reaction:

$$CO + H_2O \xrightleftharpoons[\text{highT: }rev.WGS]{\text{lowT: }WGS} CO_2 + H_2 \tag{R$2_{\text{f,r}}$}$$

Where the f and r subscripts indicate the forward and reverse reaction respectively. Summation of R1 and 3×R2_{f} yields the ideal complete steam reforming of glycerol:

$$C_3H_8O_3 + 3H_2O \rightarrow 3CO_2 + 7H_2$$

The above reaction implies that the H_2 purity in the dry syngas achievable through the conventional steam reforming of glycerol cannot exceed 70%.

At low temperatures, some hydrogen is also lost via the methanation of CO, but the reverse reaction of methane steam reforming prevails at higher temperatures:

$$CO + 3H_2 \xrightleftharpoons[\text{highT: methane steam ref}]{\text{lowT: CO methanation}} CH_4 + H_2O \tag{R$3_{\text{f,r}}$}$$

Possible reactions could also involve carbon formation:

$$2CO \xrightleftharpoons[\text{highT: rev Boudouard}]{\text{lowT: Boudouard}} CO_2 + C_S \tag{R$4_{\text{f,r}}$}$$

$$CH_4 \xrightleftharpoons[\text{lowT: carbon methanation}]{\text{highT: thermal decomp of methane,coking}} C_S + 2H_2 \tag{R$5_{\text{f,r}}$}$$

$$H_2O + C_S \xrightleftharpoons[\text{lowT: coking}]{\text{highT: steam gasif of carbon}} CO + H_2 \tag{R$6_{\text{f,r}}$}$$

Zhang et al. reported that glycerol conversion to CH_4 is highly favourable during the steam reforming process (Zhang, et al., 2007). CH_4 is obviously not a desirable product in the case of H_2 production, and thus the catalyst should have a sufficient capacity for reforming the produced CH_4 into hydrogen (R3_{r}).

As a result, the product synthesis gas is a mixture of the above gases. In the conventional process, this mixture is separated to give a hydrogen product and a concentrated carbon dioxide stream which can be captured and sequestered.

The glycerol conversion calculation for the experiments without CO_2 sorbent is based on carbon molar outflow of the gas products and the glycerol molar inflow of the reactor:

$$x_{gly}(\%) = \frac{\dot{n}_{gly,in} - \dot{n}_{gly,out}}{\dot{n}_{gly,in}} \times 100 = \frac{\dot{n}_{dry,out} \sum y_{c,out}}{3\dot{n}_{gly,in}} \times 100 \qquad (1)$$

where '$\dot{n}$'and 'y' are the relevant molar flows (mol min^{-1}) and gas mol fractions respectively, and $\dot{n}_{dry,out}$ is the dry total molar flow of gas products leaving the reactor calculated through an elemental balance of nitrogen:

$$\dot{n}_{dry,out} = \frac{\dot{n}_{N2,in}}{y_{N2,out}} = \frac{\dot{n}_{N2,in}}{\left(1 - \sum_{\text{all dry gas products}} y_i\right)} = \frac{\dot{n}_{N2,in}}{\left(1 - \left(y_{H2} + y_{CO2} + y_{CO} + y_{CH4}\right)\right)} \qquad (2)$$

Equation 2 assumes no other significant dry gases than H_2, CO_2, CO and CH_4 evolved from the reactor, and so the balance is N_2. This was checked using sporadic off-line GC-FID analysis of CH_4, C_2H_4, C_2H_6, C_3H_6, C_3H_8, C_4H_8 and C_4H_{10} for the reactor experiments at 400°C, the condition most likely to yield hydrocarbon gases other than methane. These revealed C_2H_6 in concentrations at most of 1/3 of methane's, and the remaining hydrocarbons in concentrations less than 1/9 of methane's. As methane was more accurately measured on-line and was detected at 400°C in small concentrations, and decreased further at higher temperatures. Hydrocarbons other than CH_4 were therefore neglected from the balances at the four temperatures studied and the assumption for Eq. 2 was verified.

The conversion of steam is given by:

$$x_{H2O}(\%) = \frac{\dot{n}_{H2O,conv}}{\dot{n}_{H2O,in}} \times 100 = \frac{\dot{n}_{dry,out}\left(y_{H2} + 2y_{CH4}\right) - 4x_{gly}\dot{n}_{gly,in}}{\dot{n}_{H2O,in}} \tag{3}$$

which is based on the hydrogen elemental balance (on a 2H basis) whereby the molar outflow of H-containing species leaving the reactor (other than H_2O) is balanced by the molar flow of hydrogen converted from the glycerol and water feeds.

H_2 selectivity (%) in steam reforming of glycerol is defined as:

$$H_2, Sel(\%) = \frac{2\dot{n}_{H2,out}}{2x_{H2O}\dot{n}_{H2O,in} + 8x_{gly}\dot{n}_{gyl,in}} \times 100 \tag{4}$$

H_2 purity was calculated by the ratio of H_2 volume fraction to the sum of the volume fractions of H_2, CO, CO_2 and CH_4 at the outlet. In the experiments with the CO_2 sorbent, the glycerol conversion cannot be calculated on the basis of Eqs 1 and 2, as the carbon products include the solid carbonate and the latter is not quantifiable as a time-dependent parameter in the described setup. This is why the experimental results with the CO_2-sorbent do not report glycerol or steam conversions, but are presented in terms of H_2 purity.

3. Results and discussion

3.1 Steam reforming of glycerol in absence of CO_2 removal

Figures 2a-d plot the product concentrations as a function time-on-stream in the absence of CO_2-sorbent. The H_2 selectivity and purity are shown in Fig. 3 alongside the conversions of glycerol and steam. The values reported in Figs 2 and 3 can be compared with their theoretical counterparts calculated with the thermodynamic equilibrium code EQUIL from the CHEMKIN package (Kee, et al., 1980) for which the products species CO, CO_2, H_2, and CH_4 were assumed. For instance, experimental glycerol conversions (Fig. 3) are 63%, 95%, 100% and 100% at 400, 500, 600 and 700°C respectively, whereas 100% equilibrium conversions are predicted with the code EQUIL at these four temperatures. With regard to steam conversion, values of 15.6%, 22.7%, 23.6% and 23.0% found experimentally compared well with the calculated equilibrium values of 12.6%, 24.8%, 24.8% and 21.9% at 400, 500, 600 and 700°C. A previous study using a Thermal Gravitational Analyser (TGA) showed that, in the absence of catalyst and steam, thermal decomposition of glycerol may achieve 98% conversion above 260°C under N_2 flow, and that the products include CH_4, CO_2, H_2O and volatiles (Dou et al., 2009). Thus, high glycerol conversion may or may not be caused by an active catalyst in glycerol steam reforming. In contrast, the steam conversion in addition to the glycerol conversion provides a more accurate reflection of catalyst activity in the steam reforming of glycerol. The high steam conversions obtained in the present study, found close to the equilibrium values indicate conditions close to the predicted equilibrium for 400-700°C and a catalyst with high activity. Looking now at the steam reforming products distribution, the CO observed at 700°C was the highest, as the reverse water gas shift (WGS) ($R2_r$) is favoured at high temperatures. The experimentally observed ratio of CO/CO_2 was of 0.417 at 700°C, while at 600°C, 500°C and 400°C, the ratios were respectively 0.244, 0.029, and ca. 0. These need comparing with the variably larger calculated thermodynamic equilibrium values of 0.5199, 0.338, 0.1649, and 0.036 respectively. The largest discrepancy is noted for 500°C, where the measured CO/CO_2 of 0.029 is significantly lower than the expected 0.165 from equilibrium calculations, at odds with an experimentally obtained H_2O conversion at slightly lower than its equilibrium value (22.7% compared to 24.8%). Considering now the CH_4/CO_2 ratio, the experimental values were respectively 0.25, 0.077, 0.016, and 0 at 400°C, 500°C, 600°C and 700°C, compared to the theoretical equilibrium values of 0.442, 0.077, 0.003 and 0. Surprisingly, the experimental and equilibrium CH_4/CO_2 ratios at 500°C are identical, and therefore the discrepancy in CO/CO_2 ratio at this temperature needs to be examined in the light of the assumptions made for the equilibrium calculations which do not involve CH_4 formation and removal. The carbon containing products assumed in the calculations were CO, CO_2 and CH_4 and neglected solid carbon, as no thermodynamic data on solid carbon deposited on the Ni catalyst was available, this being very different from the well known carbon graphite's thermodynamic data. The Boudouard reaction $2CO \rightarrow CO_2 + C_S$ ($R4_f$) may have been active at 500°C and would not have been accounted for in the thermodynamic equilibrium calculations, resulting in the lower CO/CO_2 ratio found experimentally. Considering the discrepancy in CH_4/CO_2 experimental and equilibrium ratios at 400°C (0.25 compared to 0.442), it could also have been caused by the absence of solid C in the equilibrium predictions. The presence of solid C at 400°C was corroborated by SEM images and their corresponding EDX analysis. SEM images of the morphology of the fresh and reduced catalysts exhibited two kinds of morphologies: large crystallites of several hundred nm size and smaller ones of less than 100 nm size. Little difference could be seen between the fresh and the reduced catalysts. The EDX spectrum indicated the Al, Ni and O contained in the samples, with the expected slightly smaller O peak in comparison to that of Al, obtained for the reduced catalyst. The SEM image of the catalyst after steam reforming reaction at 400°C showed a very different morphology than that of the fresh or reduced catalyst. It exhibited carbon structures, confirmed by a carbon peak in the EDX spectrum, some flat-like irregular disc shapes, other curved tubular shapes of around 100 nm size, believed to be filamentous carbon, as well as smaller spherical shapes entirely covering the catalyst surface whereas the larger crystallites observed on the reduced catalyst were no longer visible. This low temperature would have seen a low activity in steam methane reforming but a significant one for methane thermal decomposition producing carbon deposits (R_{5f}), resulting in a low measurement of CH_4/CO_2 not reflected in the calculated equilibrium ratio. Coking, due to polymerisation, thermal decomposition and other reactions, occurs if the gas does not contain enough oxidizing component such as H_2O or if the reaction temperature of steam reforming reaction is too low, leading to blockage of catalyst pores and in extreme cases complete failure of the reactor (Slinn, et al., 2008).

The results in Fig. 3 show that H_2 selectivity is greatly increased with increasing temperatures. The best H_2 purity achieved was 68% at 600°C. As indicated by the small presence of the by-products CO and CH_4 at the four temperatures studied, the H_2 purity never quite reached the theoretical equilibrium value of 70%, which would have reflected both ideal glycerol and steam conversions. The low CH_4 and high H_2 purity suggest that methane steam reforming (R_{3r}) was active in the 500-700°C range. Some studies indicated that the reactions of glycerol steam reforming at lower temperatures are strongly dependent on the capacity of the active metals for breaking the C-C bond, and with a further increase in temperature to above 400°C, the concentrations of reaction intermediates such as acetaldehyde over the catalyst decreased rapidly, where H_2, CO_2, CH_4 and CO became the only products and H_2 concentration was increased greatly (Zhang, et al., 2007). They also reported results similar to ours in that steam reforming of glycerol resulted in a rapid decrease of methane concentration and methane became negligible above 500°C.

3.2 Glycerol steam reforming with in-situ CO_2 removal

Although the glycerol steam reforming has in the past been carried out for H_2 production, as stated previously, there is room for development of this process using *in-situ* CO_2 removal. In the case of addition of a CO_2 acceptor to the reactor, carbon dioxide is converted to a solid carbonate and thereby could directly produce higher purity H_2 than a conventional catalyst-only reactor. Regeneration of the sorbent releases relatively pure CO_2 suitable for sequestration. Internal carbon dioxide removal will also add extra heat to the reforming reaction due to the exothermicity of CO_2 chemisorption on the sorbent. When using the CO_2 sorbent and due to the fixed amount of sorbent in an experimental run, the CO_2 concentration in the product gas (c_{CO_2}) rises rapidly once the sorbent reaches a certain capacity (q). This is termed CO_2 breakthrough (Dou et al., 2003). In this study, we defined breakthrough as CO_2 outlet concentration of 10% of the maximum CO_2 concentration in product gas (c_{0,CO_2}). The 10% was arbitrarily chosen to define breakthrough as this corresponded to an absolute CO_2 concentration of 3% measured in the dry syngas, thus presenting a small enough but nevertheless accurately measurable concentration.

Typical product distributions for glycerol steam reforming with *in-situ* CO_2 removal at different temperatures are shown in Fig. 4a-d. As can be seen from the figures, with an increase in the time-on-stream, there is a gradual deterioration of CO_2 removal as the sorbent begins to saturate. Eventually the process degrades to the conventional catalyst-only behaviour, and the compositions of the product gases approach their stable values. When compared with the data in the absence of the sorbent, the only significant difference is found for H_2 at 400°C, where a lower H_2 concentration is obtained. It may therefore be that the presence of the saturated sorbent intimately mixed with the Ni catalyst hinders the latter's activity at 400°C, perhaps by impeding the CH_4 thermal decomposition reaction. The hydrogen purity as a function of time at different temperatures is shown in Fig. 5. As shown in Fig. 5, the maximum H_2 purity is, as expected, obtained in the pre-CO_2 breakthrough periods. The maximum H_2 purity of 97% was recorded at 500°C for three minutes, followed closely by 94% at 600°C for four minutes. The operation durations for producing high purity hydrogen of more than 90% were 3.6, 6.8 and 5 min for the three temperatures of 400°C, 500°C and 600°C respectively. The times of operation associated high H_2 purity are consistent with the CO_2 breakthrough times. At 700°C, the maximum H_2 purity was only 77% and the CO_2 breakthrough time was 0.7 min, indicating a poor effect for CO_2 removal resulting in little sorption enhancement of the steam reforming. This is explained by reaching temperatures carbonate decomposition (calcinations) in the presence of steam is significantly active. The calcined dolomite has also a certain affinity towards steam as follows (Barelli, et al., 2008):

$$CaO + H_2O \rightarrow Ca(OH)_2 \qquad \text{R7}$$

Steam may not solely react with glycerol according to the reforming reaction. Reaction R7 may have affected the actual H_2O/glycerol ratio in the reactor. The overall reaction of glycerol steam reforming can be represented by:

$$C_3H_8O_3 + 3H_2O \rightarrow 3CO_2 + 7H_2 \qquad \text{R1+3×R2}_f$$

As mentioned previously, according to the above reaction, complete steam reforming of glycerol could provide a product gas with a maximum H_2 purity of 70% in absence of CO_2 sorbent. In all the present experiments of glycerol steam reforming with *in-situ* CO_2 removal, the H_2 purity was substantially higher than this limit for a significant period of operation preceding the sorbent saturation, validating the concept of sorption-enhancement for glycerol steam reforming. It seems that the reaction temperature of 500°C is an optimum temperature for glycerol steam reforming with *in-situ* CO_2 removal, exhibiting the longest CO_2 breakthrough time and the highest H_2 purity.

The CO_2 removal process during glycerol steam reforming in a fixed-bed reaction system is considered to be a very complex phenomenon involving a large number of sub-processes. The CO_2 breakthrough curve of a fixed-bed reactor roughly followed an *S* shape, which shows the active part of the fixed bed where reaction actually takes place, resulting in a gradient in CO_2 concentration in the product gas from zero to equilibrium. This process is modelled here with the following assumptions (Wang, et al., 1996 and Dou, et al., 2003): (i) the fixed-bed is isothermal; (ii) gas velocity is constant; (iii) plug flow conditions for the gas phase is without axial dispersion, implying the use of a one-dimensional model along the reactor axis, *z*; (iv) the gas phase is ideal. The modelling of the fixed-bed reactor is based on the conservation equation derived from the mass balance on the fluid and solid phase. A typical constant pattern model for fixed-bed reactor is represented by Eq. 5 (Wang, et al., 1996; Dou, et al., 2003; 2005 and 2006):

$$\frac{c_{CO_2}}{c_{0,CO_2}} = \frac{q}{q_0} = x_{CO_2} \qquad (5)$$

where x_{CO_2} is the sorbent's conversion and q_0 represents the capacity of sorbent in equilibrium adsorbing condition. Note q_0 may be lower than the theoretical maximum capacity of the sorbent ($q_{0,th}$), which can be estimated from the dolomite composition, assuming all the CaO present in the calcined sorbent forms carbonate. As the content of CaO is 30.7%, the maximum theoretical capacity for CO_2 capture is estimated as 24.087g per 100g of calcined dolomite.

If the CO_2 removal is controlled by the chemical rate of conversion at the particle surface, then the data can be modelled through the use of the shrinking core model expression (Barelli, et al., 2008; Dou, et al., 2003 and 2005), also called ‘contracting volume’ model. The time required for particle conversion is given by:

$$g(x) = \frac{t - t_b}{\tau_g} = 3\left(1 - (1 - x_{CO_2})^{1/3}\right) \tag{6}$$

where τ_g represents the characteristic time required for the complete conversion of the particle, the breakthrough time is t_b. We modelled the data using x_{CO_2} vs. t from the CO_2 breakthrough curves within the conversions of 0.10-0.83 for the four constant temperature experiments.

On the basis of the model and experimental results, a linear fit between $[1-(1-x_{CO_2})^{1/3}]$ and time, expressed by Eq. 6 and shown in Fig. 6, yields the characterisitic time τ_g. The values of τ_g for each temperature are listed in Table 1 alongside the correlation coefficient. Goodness of fit was observed at all temperatures, which indicated the reaction rate of the sorbent with CO_2 was mainly controlled by the surface chemical reaction. In addition, other models were tested and the linear fits were compared to that of the shrinking core model. These included:

(i) contracting surface $g(x)=2[1-(1-x)^{0.5}]$,

(ii) 3D-diffusion $g(x)=[1-(1-x)^{1/3}]^2$,

(iii) 2D diffusion $g(x)=x+(1-x)\ln(1-x)$

(iv) 1D-diffusion models $g(x)=x^2$

In the case of the 700°C data, the 1D-diffusion model exceeded very slightly the goodness of fit found with the shrinking core model. At 400°C, and using a larger range of data, including higher conversions of the calcined dolomite to its carbonate, the 1D diffusion model also provided a slightly higher correlation coefficient. All the other models generated worse fits.

The shrinking core model's description of the gas-solid reaction kinetics assumes that the reaction zone is restricted to a thin front advancing from the outer surface into the particle. The reaction is unlikely to be controlled by the gas-film mass transfer; therefore, the rate-limiting steps should be the chemical reaction or the carbonate product layer diffusion, or both (Barelli, et al., 2008; Dou, et al., 2003 and 2005). The close agreement of the two models (shrinking core and 1D-diffusion) indicates that the reaction would have been controlled by both surface reaction kinetics and 1D diffusion through the carbonate layer, with the latter being more likely at higher conversions of the sorbent, and higher temperatures. The present study is of course limited in its investigation of calcined dolomite as an *in-situ* CO_2 sorbent of glycerol steam reforming. Issues related to the regenerability of the sorbent, its stability as it undergoes many cycles of carbonation-decomposition, need to be addressed. However the proof of concept of sorption enhanced steam reforming of glycerol is evident in the results presented here and offers a good basis for more thorough investigation of this process in the future.

4. Conclusions

Sorption-enhanced seam reforming of glycerol was found to be an effective means for achieving hydrogen purity exceeding 90% and decreasing CO_2 concentration. The effect of temperature in the 400-700°C on the products selectivity is strong, with a H_2 selectivity that increases with increasing the temperature. The experimental results using a calcined dolomite sorbent showed that 500°C was an optimum temperature with the longest CO_2 breakthrough time and the highest H_2 purity of 97%. The shrinking core model applied to the CO_2-sorption, and the 1D-diffusion model at higher temperatures and conversions agreed well with the data, indicating a sorption mechanism controlled both by surface kinetics and 1D-diffusion through the carbonate layer.

Acknowledgments

The Engineering and Physical Sciences Research Council, UK, is gratefully acknowledged for funding of work through grant EP/F027389/1. Our thanks also go to Dr Martyn V. Twigg, Johnson Matthey for providing the reforming catalyst, and Mr James Wylie, WBB Minerals, for the (Warmsworth quarry) dolomite.

References

Adhikari, S., Fernando, S.D., Gwaltney, S.R., To, S.D.F., Bricka, R.M., Steele, P.H., Haryanto, A., 2007a. A thermodynamic analysis of hydrogen production by steam reforming of glycerol. International Journal of Hydrogen Energy 32, 2875-2880.

Adhikari, S., Fernando, S., Haryanto, A., 2007b. Production of hydrogen by steam reforming of glycerine over alumina-supported metal catalysts. Catalysis Today 129, 355–364.

Adhikari, S., Fernando, S.D., To, S.D.F., Bricka, R.M., Steele, P.H., Haryanto, A., 2008. Conversion of glycerol to hydrogen via a steam reforming process over nickel Catalysts. Energy & Fuels 22, 1220-1226.

Balasubramanian, B., Ortiz, A.L., Kaytakouglu, S., Harrison, D.P., 1999. Hydrogen from methane in a single-step process. Chem. Eng. Sci. 54, 3543-3552.

Barelli, L., Bidini, G., Gallorini, F., Servili, S., 2008. Hydrogen production through sorption-enhanced steam methane reforming and membrane technology: A review. Energy 33, 554-570.

Czernik, S., French, R., Feik, C., Chornet, E., 2002. Hydrogen by catalytic steam reforming of liquid byproducts from biomass Thermoconversion Processes. Ind. Eng. Chem. Res. 41, 4209-4215.

Ding, Y., Alpay, E., 2000. Adsorption-enhanced steam methane reforming. Chemical Engineering Science 55, 3929-3940.

Dou, B., Chen, B., Gao, J., Sha, X., 2005. Reaction of solid sorbents with hydrogen chloride gas at high temperature in a fixed-bed reactor. Energy & Fuels 19, 2229-2234.

Dou, B., Chen, B., Gao, J., Sha, X., 2006. HCl removal and chlorine distribution in the mass transfer zone of a fixed-bed reactor at high temperature. Energy & Fuels 20, 959-963.

Dou, B., Dupont, V, Williams, P.T., Chen, H., Ding, Y., 2009. Thermogravimetric kinetics of crude glycerol. Bioresource Technology. doi:10.1016/j.biortech.2008.11.037. (In Press, Corrected Proof, Available online 22 January 2009)

Dou, B., Dupont, V, Williams, P.T., 2008. Computational fluid dynamics simulation of gas-solid flow during steam reforming of glycerol in a fluidised bed reactor. Energy & Fuels 22, 4102–4108.

Dou, B., Gao, J., Baek. S.W., Sha, X. 2003. High-temperature HCl removal with sorbents in a fixed-bed reactor. Energy & Fuels 17, 874-878.

Douette, A.M.D., Turn, S.Q., Wang, W., Keffer, W.I., 2007. Experimental Investigation of Hydrogen Production from Glycerin Reforming. Energy & Fuels 21, 3499-3504.

Dupont, V., Ross, A.B., Hanley, I., Twigg, M.V., 2007. Unmixed steam reforming of methane and sunflower oil: a single reactor process for H2-rich gas. International Journal of Hydrogen Energy 32, 67-79.

Dupont, V., Ross, A.B., Knight, E., Hanley, I., Twigg, M.V., 2008. Production of hydrogen by unmixed steam reforming of methane. Chemical Engineering Science 63, 2966-2979.

Essaki, K., Muramatsu, T., Kato, M., 2008. Effect of equilibrium shift by using lithium silicate pellets in methane steam reforming. International Journal of Hydrogen Energy 33, 4555-4559.

Harrison, D.P., 2008. Sorption-enhanced hydrogen production: A review. Ind. Eng. Chem. Res. 47, 6486-6501.

Hirai, T., Ikenaga. N.O., Miyake. T., Suzuki, T., 2005. Production of hydrogen by steam reforming of glycerin on ruthenium catalyst. Energy & Fuels 19, 1761-1762.

Kee, R.J., Miller, J.A., Jefferson, T.H., 1980. CHEMKIN: A general purpose problem-independent, transportable, FORTRAN Chemical Kinetics Code Package. Sandia National Laboratories Report SAND80-8003.

Kinoshita, C.M., Turn,S.Q., 2003. Production of hydrogen from bio-oil using CaO as a CO2 sorbent. International Journal of Hydrogen Energy 28, 1065-1071.

Lee, K.B., Beaver, M.G., Caram, H.S., Sircar, S., 2007. Novel thermal-swing sorption-enhanced reaction process concept for hydrogen production by low-temperature steam-methane reforming. Ind. Eng. Chem. Res. 46, 5003-5014.

Lee, K.B., Beaver, M.G., Caram, H.S., Sircar, S., 2008. Production of fuel-cell grade hydrogen by thermal swing sorption enhanced reaction concept. International Journal of Hydrogen Energy 33, 781-790.

Li, Z.S., Cai, N.S., 2007. Modeling of Multiple Cycles for sorption-enhanced steam methane reforming and sorbent regeneration in fixed bed reactor. Energy & Fuels 21, 2909-2918.

Ma, F., Hanna, M.A., 1999. Biodiesel production: a review. Bioresource Technology 70, 1-15.

Mayorga, J.R., Sircar, S., 1999. Sorption-enhanced reaction process for hydrogen production. AIChE J. 45, 248-256.

Slinn, M., Kendall, K., Mallon, K., Andrews, J., 2008. Steam reforming of biodiesel by-product to make renewable hydrogen. Bioresource Technology 99, 13, 5851-5858.

Wang, W.Y., Ye, Z.C., Bjerle, I., 1996. The kinetics of the reaction of hydrogen chloride with fresh and spent Ca-based desulfurization sorbents. Fuel 75, 207-212.

Yi, K.B., Harrison, D.P., 2005. Low-pressure sorption-enhanced hydrogen production. Ind. Eng. Chem. Res. 44, 1665-1669.

Zhang, B., Tang, X., Li, Y., Xu, Y., Shen, W., 2007. Hydrogen production from steam reforming of ethanol and glycerol over ceria-supported metal catalysts. International Journal of Hydrogen Energy 32, 2367-2373.

Table 1. Characteristic times τ_g of *in-situ* CO_2 removal derived from Eq. 6, goodness of linear fit is represented by closeness to 1 of correlation coefficient *R*.

Temperature (°C)	τ_g **(min)**	***R***
400	11.73	0.9655
500	5.26	0.9921
600	10.9	0.9975
700	3.43	0.9898

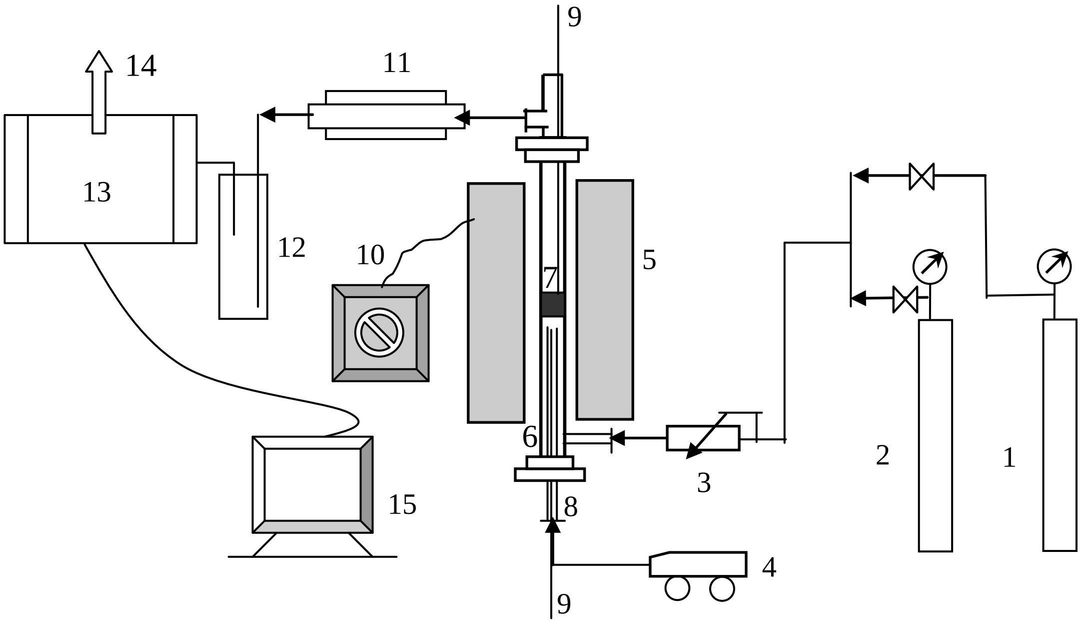

Fig.1. Schematic diagram of the experimental setup.

1, N_2 cylinder; 2, H_2 cylinder; 3, Mass flow controller for N_2 feed; 4, Syringe pump and feed injector (liquid water-glycerol mix); 5, Oven; 6, Reactor; 7, catalyst with or without sorbent; 8, Injector; 9, Thermocouple; 10, Temperature controller; 11, Condenser; 12, Silica gel; 13, Gas analyser; 14, Outlet; 15, Computer

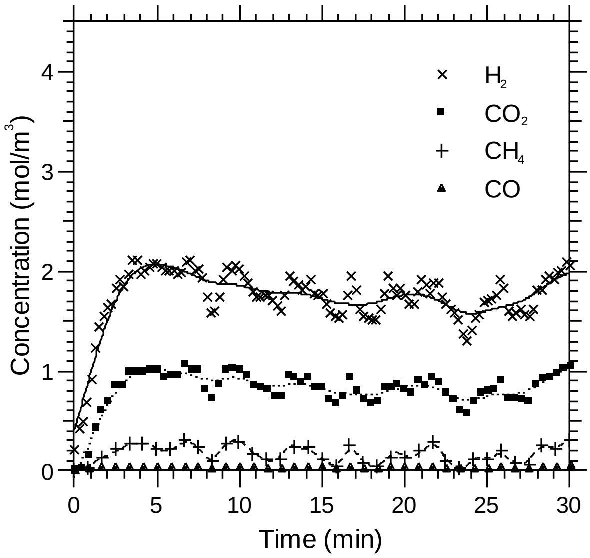

H₂
CO₂
CH₄
CO
Concentration (mol/m³)
Time (min)
0
1
2
3
4
0
5
10
15
20
25
30

(a)

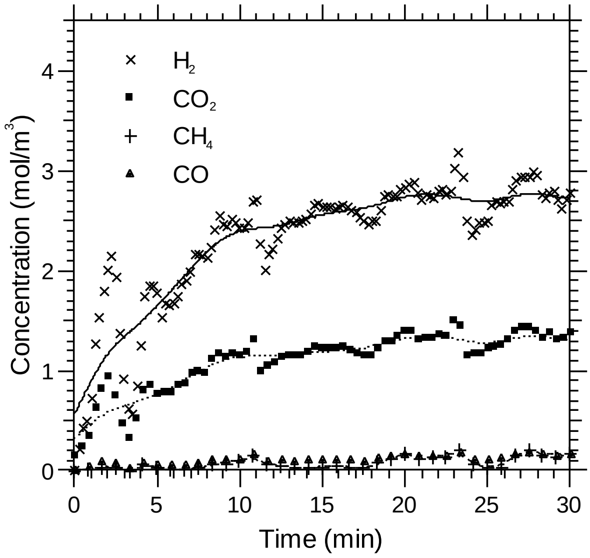

H₂
CO₂
CH₄
CO
Concentration (mol/m³)
Time (min)
0
1
2
3
4
0
5
10
15
20
25
30

(b)

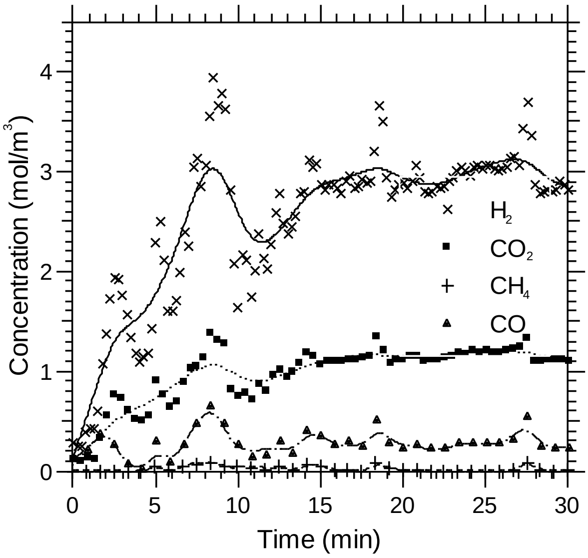

(c)

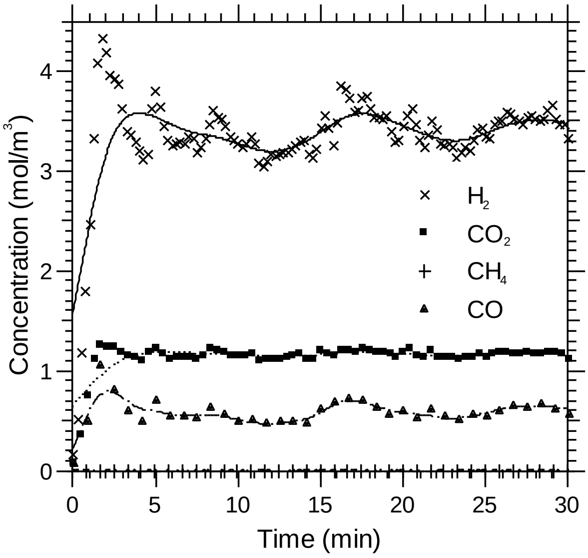

(d)

Fig. 2 Product gases distribution of glycerol steam reforming at different temperatures, (a), 400°C; (b), 500°C; (c), 600°C; (d), 700°C.

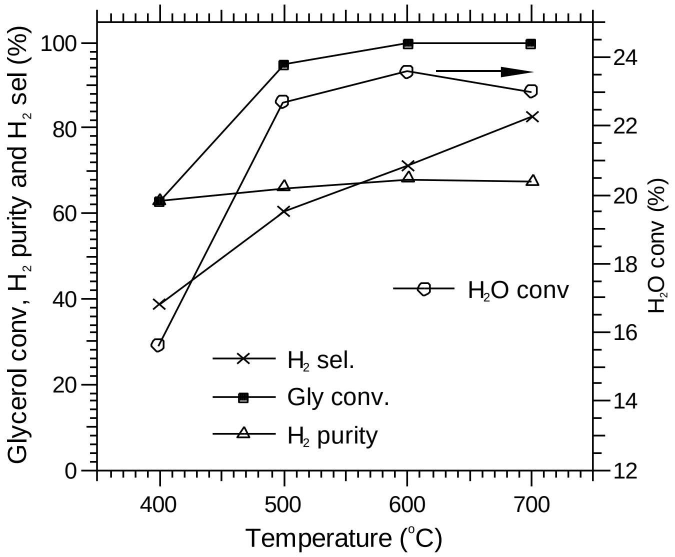

Fig. 3 H_2 selectivity, H_2 purity, glycerol (left scale) and steam conversions (right scale) at different temperatures.

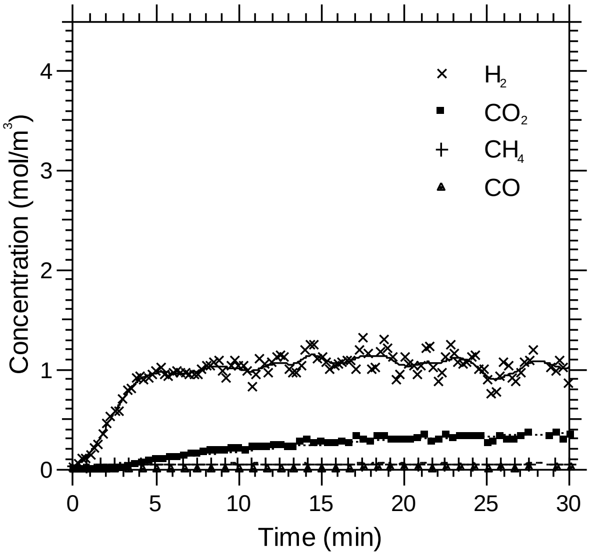

Concentration (mol/m³)
Time (min)
0
1
2
3
4
0
5
10
15
20
25
30
× H_2
■ CO_2
+ CH_4
▲ CO

(a)

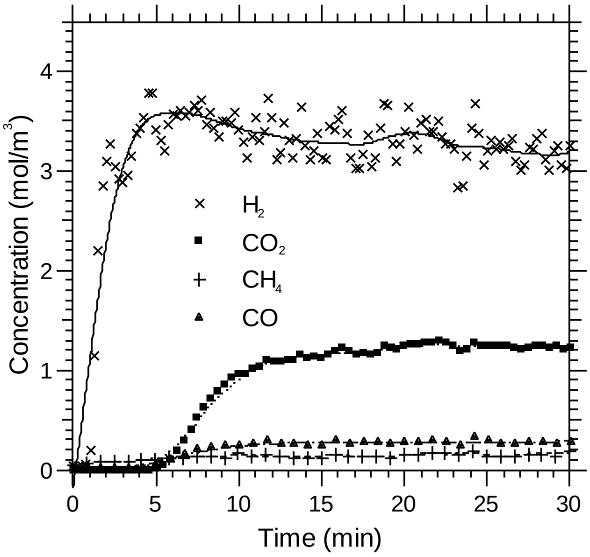

Concentration (mol/m³)
Time (min)
0
1
2
3
4
0
5
10
15
20
25
30
× H_2
■ CO_2
+ CH_4
▲ CO

(b)

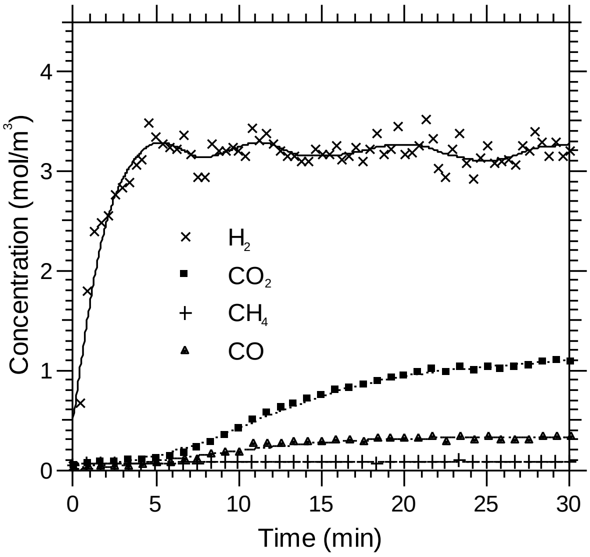

(c)

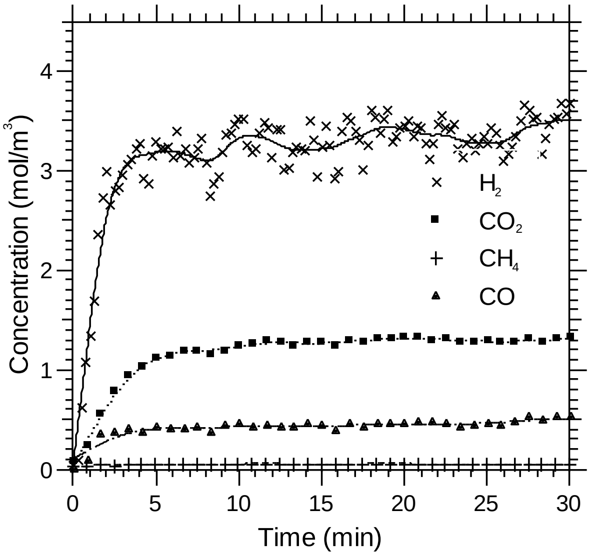

(d)

Fig. 4 Product gases distribution of glycerol steam reforming with in-situ CO_2 removal at different temperatures, (a), 400°C; (b), 500°C; (c), 600°C; (d), 700°C.

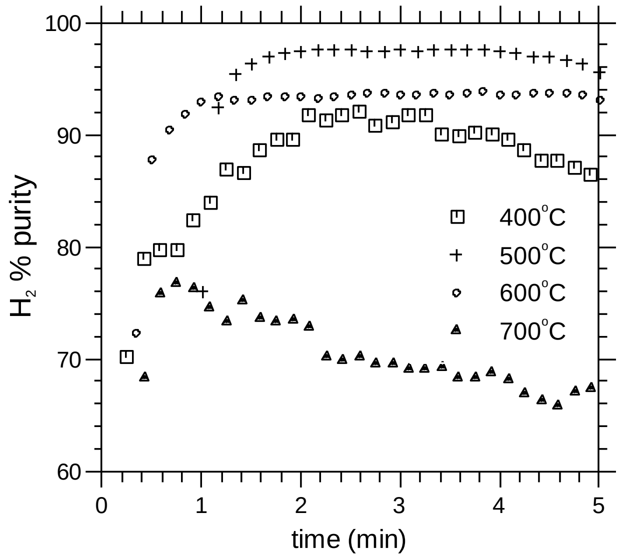

Fig. 5 H_2 purity as a function of time at different temperatures. Density of scatter points shown for each curve is of one in two.

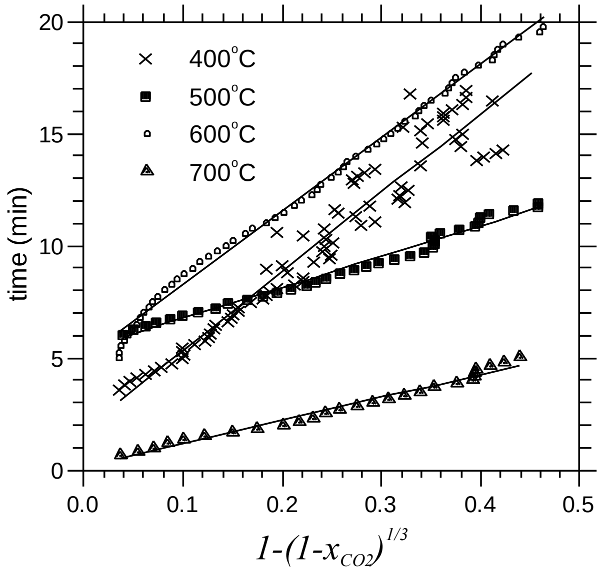

Fig. 6 Relationship between 1-(1-x_{CO2})$^{1/3}$ and time. The straight lines illustrate the validity of Eq. 6, yielding characteristic time τ_g listed in Table 1.